Research Article

Dermatology Journal of Cosmetic and Laser Therapy

# Identification and Validation of A Ten Cuproptosis-Related Lncrna Prognostic Signature for Stomach Adenocarcinoma

**Qi Ma[1], Yuan Hui[1], Bin Feng Yang[2], Jing Xian Li[1], Da You Ma[1], Bang Rong Huang[2]***

[1]*School of Integrative Medicine, Gansu University of Traditional Chinese Medicine, Lanzhou, China*

[2]*Department of Oncology, Gansu Provincial Hospital of Traditional Chinese Medicine, Lanzhou, China*

***Corresponding Author**

Bang Rong Huang, Department of Oncology, Gansu Provincial Hospital of Traditional Chinese Medicine, Lanzhou, 730050, China.

**Submitted:** 07 Dec 2022; **Accepted:** 14 Dec 2022; **Published:** 20 Dec 2022

**Citation:** Ma, Q., Hui, Y., Yang, B. F., Li, J. X., Ma, D. Y., et al. (2022). Identification and Validation of A Ten Cuproptosis-Related Lncrna Prognostic Signature for Stomach Adenocarcinoma. *Dearma J Cosmetic Laser Therapy,* 1(1), 42-53.

## *Abstract*

***Background:*** *Cuproptosis is a recently discovered method of copper-induced cell death that serves an essential part in the progression and spread of stomach adenocarcinoma (STAD). Multiple studies have found that lncRNAs, or long non-coding RNAs, are strongly correlated with the outcome for STAD patients. However, the nature of the connection between cuproptosis and lncRNAs in STAD is still not completely understood. Our study set out to create a predictive hallmark of STAD based on lncRNAs associated with cuproptosis, with the hope that this would allow for more accurate prediction of STAD outcomes.*

***Methods:*** *We retrieved the transcriptional profile of STAD as well as clinical information from The Cancer Genome Atlas (TCGA). The cuproptosis-related genes (CRGs) were gathered through the highest level of original research and complemented with information from the available literature. We constructed a risk model using co-expression network analysis, Cox regression analysis, and least absolute shrinkage and selection operator (LASSO) analysis to identify lncRNAs associated with cuproptosis, and then validated its performance in a validation set. Survival study, progression-free survival analysis (PFS), receiver operating characteristic (ROC) curve analysis, Cox regression analysis, nomograms, clinicopathological characteristic correlation analysis, and principal components analysis were used to evaluate the signature's prognostic utility. Additionally, ssGSEA algorithms, KEGG, and GO were employed to assess biological functions. The tumor mutational burden (TMB) and tumor immune dysfunction and rejection (TIDE) scores were utilized in order to evaluate the effectiveness of the immunotherapy.*

***Results:*** *In order to construct predictive models, nine distinct lncRNAs (AC087521.1, AP003498.2, AC069234.5, LINC01094, AC019080.1, BX890604.1, AC005041.3, DPP4-DT, AL356489.2, AL139147.1) were identified. The Kaplan-Meier and ROC curves, which were applied to both the training and testing sets of the TCGA, provided evidence that the signature contained a sufficient amount of predictive potential. The signature was shown to contain risk indicators that were independent of the other clinical variables, as demonstrated by the findings of a Cox regression and a stratified survival analysis. The ssGSEA study provided additional evidence that predictive variables were highly connected with the immunological condition of STAD patients. Surprisingly, the combination of high risk and high TMB reduced survival time for patients. A worse prognosis for the immune checkpoint blockade response was also suggested by the fact that patients in the high-risk group had higher TIDE scores.*

***Conclusion:*** *The potential clinical uses of the identified risk profiles for the 10 cuproptosis-related lncRNAs include the assessment of the prognosis and molecular profile of STAD patients and the creation of more targeted therapy strategies.*

**Keywords:** Cuproptosis, Lncrna, Stomach Adenocarcinoma, Prognosis, TCGA, TMB

## Introduction

There are over a million new cases of stomach cancer each year, making it a global health emergency [1]. Even though the rates of both new cases and fatalities from gastric cancer are falling, each year more than a million people are diagnosed and approximately 760,000 lose their lives to the disease around the world [2]. Stomach adenocarcinoma is the most prevalent histological subtype of GC. Despite advances in treatment, such as systemic chemotherapy, radiation, surgery, immunotherapy, and targeted therapy, the overall survival rate for persons with STAD remains unsatisfactory [3, 4]. Increasing data suggests that multigene signatures can be used to stratify risk and predict outcome in STAD [5-8]. For this reason, our goal is to identify a set of lncRNAs that are significantly correlated with cuproptosis and utilize this information to make predictions about patients' overall survival following STAD diagnosis.

Physiological processes that rely on copper include energy metabolism, autophagy, and the response to oxidative stress [9]. But if the amount of copper in the body rises above what homeostatic processes can handle, it could be hazardous [10]. Copper levels are significantly elevated in the blood and tumor tissues of cancer patients, and this has been demonstrated to encourage tumor development and spread [11, 12]. Newly discovered copper-induced cell death was given the name "cuproptosis" in a study that appeared in the journal Science [13]. As a result of forming a covalent bond with lipoacylated components of the tricarboxylic acid (TCA) cycle, copper induces a cascade of toxic protein stress and, ultimately, cell death [14]. This exemplifies copper's tremendous anticancer potential in fighting cancers with natural resistance to apoptosis.

In recent years, lncRNAs have gained prominence as key regulators of cellular biolog [15]. There is mounting evidence that lncRNAs play a role in cancer both as oncogenes and as tumor suppressors [16, 17]. In addition to controlling cell growth, differentiation, invasion, and metastasis, they can also alter cancer cells' metabolism [18-20]. It is unclear how copper regulates death in malignancies, and research on the function of cuproptosis-associated lncRNAs in STAD are inconsistent. Therefore, the purpose of this bioinformatics-based work is to investigate the function of lncRNAs involved in cuproptosis in STAD.

## Materials and Methods

### Data Collection

From the Cancer Genome Atlas database (TCGA, https://portal.gdc.cancer.gov), we pulled RNA sequencing data and associated clinical information for 32 normal stomach tissues and 375 stomach adenocarcinoma samples. Extracting and normalizing the RNA-seq data to the FPKM format was done in Perl (Strawberry-Perl-5.30.0.1; https://www.perl.org). The MAF-formatted mutation data came from the TCGA database. Information about the 19 genes involved with cuproptosis was gathered from both primary and secondary resources.

### Identification of Differently Expressed Cuproptosis-Associated Lncrnas

A total of 16876 lncRNAs were discovered in the TCGA-STAD RNA-seq data by employing the GTF annotation files of human lncRNAs downloaded from the GENCODE website (GENCODE, https://www.gencodegenes.org/). Additionally, Pearson correlation analysis was utilized to examine the co-expression associations between CRGs and lncRNAs in STAD samples. The threshold was set at $|\text{Coefficient}| > 0.4$ and p-value $< 0.001$.

### Establishment and Validation of A Predictive Signature for Prognosis

Utilizing the "caret" R package, the STAD samples were randomly split into a training risk set and a test risk set. The Signature of lncRNAs involved in cuproptosis were constructed using the train set and then validated using the test set and the full dataset. Predictive value of lncRNAs was evaluated utilising univariate Cox regression analysis, and LASSO regression analysis was used to choose the best collection of prognostic lncRNAs to incorporate into a model for assessing patient prognosis in STAD. The risk assessments were made using the following calculator: Riskscore= (Coef,1, *, expression, lncRNA,1) +(Coef,2, *, expression, lncRNA,2) +(Coef,n,*,expression,lncRNA,n). Based on the training set's median Risk score, which was used to classify the circumstance, the samples were labeled as low-risk or high-risk. Kaplan-Meier curves were utilized to evaluate overall mortality and progression-free survival rates between high-risk and low-risk groups of STAD patients in the training and testing sets. Area under the ROC curve (AUC) and consistency index were used to evaluate the model's prediction abilities for survival.

### Construction of A Nomogram Using Riskscore and Clinical Factors

To ascertain if the cuproptosis-related lncRNA signature had independent predictive relevance, univariate and multivariate Cox regression analysis were performed. To calculate the 1-year, 3-year, and 5-year OS probabilities for patients with STAD, we included clinical factors and used the "rms" R package to build an outcome-related prediction nomogram and accompanying calibration plots. The prediction effect was larger when the nomogram had a better prognostic ability, and the calibration curve was closer to the 45°line.

### PCA, GO, and KEGG Analysis

Principal component analysis (PCA) was used to identify the expression patterns of lncRNAs involved in cuproptosis for STAD samples, allowing us to see the distribution of high- and low-risk samples graphically. In addition, items from GO and KEGG were found by evaluating differentially expressed genes (DEGs) between high-risk and low-risk categories with the criteria of a p-value of less than 0.05 and a log2FC of greater than 1. When both the FDR and the p-value were less than 0.05, we concluded that there was significant enrichment.

### Single-Sample Immune Infiltration Level Analysis

Individual cancer samples were analyzed using the ssGSEA, which applied gene signatures expressed by immune cell types. We measured the enrichment scores of ssGSEA for distinct subsets of immune cells, related functions, or pathways in order to further investigate the association between Riskscore and these elements of the immune system.

### Tumor Mutation Burden and Tumor Immune Dysfunction and Exclusion Score

To get at the mutation information, we used the Pearl programming language after importing the somatic mutation data that we had downloaded from the TCGA website. We evaluated TMB and survival rates in high-risk and low-risk groups by assessing and merging TCGA data with the "maftools" program. For the purpose of assessing tumor immune dysfunction and exclusion, we downloaded the TIDE scoring file from the TIDE website (TIDE, http://tide.dfci.harvard.edu/). Furthermore, the IC50 values of medications currently used to treat STAD in both high- and low-risk groups were predicted using the "pRRophetic" R package.

### Statistical Analysis

The following packages were used in R software (version 4.1.3), for data analysis and visualization purposes: “tidyverse”,

"limma", "pheatmap", "survival", "survminer", "ggalluvial", "dplyr", "ggplot2", "caret", "glmnet", "timeROC", "ggExtra", "rms", "pec", "regplot", "scatterplot3d", "org.Hs.eg.db", "clusterProfiler", "enrichplot", "DOSE", "circlize", "RColorBrewer", "ComplexHeatmap", "ggpubr", "stringi", "colorspace", "GSVA", "GSEABase", "reshape2", "maftools", "pRRophetic". When the p-value was less than 0.001 or 0.05, it was considered significant.

## Results

### Prognosis-Related lncRNAs with Co Expression of Cu Proptosis

We identified 430 lncRNAs involved in cuproptosis based on a Pearson correlation analysis (|Coefficient| > 0.4 and p-value < 0.001)(Figure 1A). Following a univariate Cox analysis (p < 0.05), we identified 26 lncRNAs that were differentially expressed and found to be associated with prognosis: AC087521.1, AP003498.2, AC069234.5, NCAM1-AS1, LIMS1-AS1, LINC01094, AC090559.1, AC092042.1, AL049840.5, RHOQ-AS1, AC037198.1, DIRC1, AC019080.1, SLC6A1-AS1, AC007390.1, BX890604.1, RASGRF2-AS1, LINC01303, AC005041.3, AC006033.2, DPP4-DT, AL356489.2, AC022382.2, AL139147.1, VCAN-AS1, AC018752.1(Figure 1B).

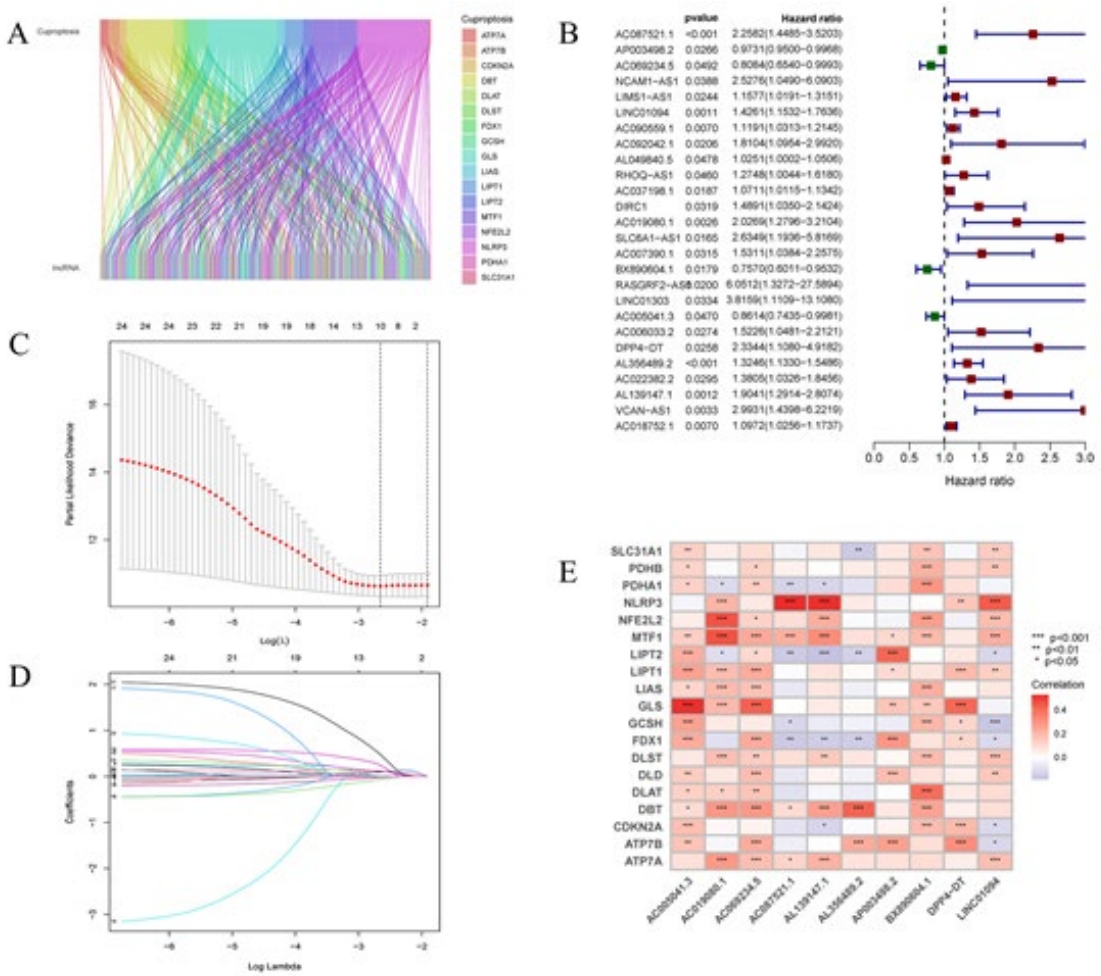


**Figure 1:** A. Genes and lncRNAs involved in cuproptosis are arranged in a Sankey diagram; B. Univariate Cox regression analysis; C. The LASSO coefficient distribution of lncRNAs related with cuproptosis; D. The 10-fold cross validation of variable selection in LASSO algorithm; E.Analysis of the relationship between lncRNAs and genes involved in cuproptosis.

### Building a Signature of lncRNAs Involved in Cuproptosis

With the help of LASSO regression analysis, we were able to develop a signature for predicting the prognosis of HCC cases. Successful incorporation of 10 lncRNAs into a risk model (Figure 1C-E). Riskscores for these ten lncRNAs (Table1) were computed by entering their respective coefficients into the following equation: riskscore = (0.1017 * AC087521.1 expression) +(-0.0042 * AP003498.2 expression) +(-0.0085 * AC069234.5 expression) + (0.1088 * LINC01094 expression) + (0.2440 * AC019080.1 expression) + (-0.0706 * BX890604.1) + (-0.0223 * AC005041.3) + (0.4741 * DPP4-DT) + (0.1234* AL356489.2) + (0.0870 * AL139147.1). To determine if a patient was at high, or low risk, we looked at their median threshold value. The high-risk group saw far higher mortality than the low-risk group across the board and in both training and validation sets (Figure 2A-L). The high-risk group also fared far worse than the low-risk group in terms of progression-free survival in the training set (Figure 3A).

**Table 1: List of lncRNAs and coefficient**

| lncRNA | coefficient |
|---|---|
| AC087521.1 | 0.1017 |
| AP003498.2 | -0.0042 |
| AC069234.5 | -0.0085 |
| LINC01094 | 0.1088 |
| AC019080.1 | 0.2440 |
| BX890604.1 | -0.0706 |
| AC005041.3 | -0.0223 |
| DPP4-DT | 0.4741 |
| AL356489.2 | 0.1234 |
| AL139147.1 | 0.0870 |

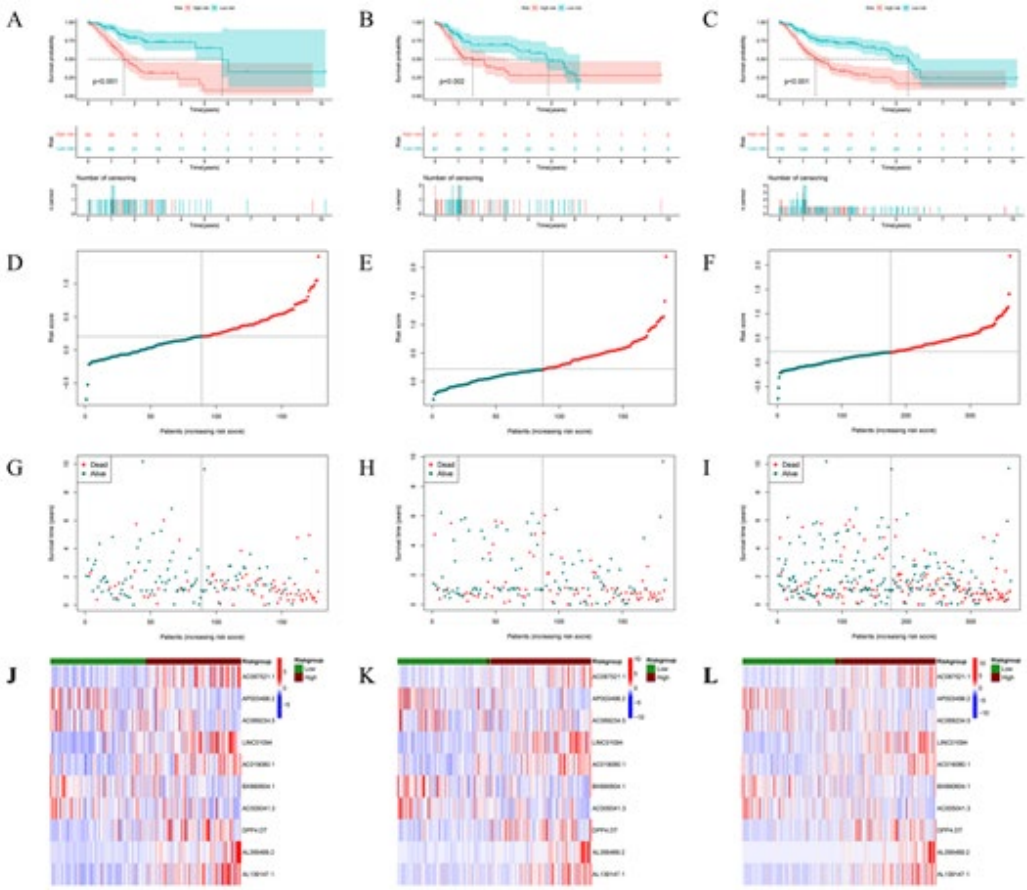


**Figure 2:** A-C. Kaplan-Meier plots of overall survival time for individuals with STAD; D-F The distribution of overall survival riskscore; G-I Survival status distribution; J-L Comparison heatmaps of train, test, and full datasets for 10 lncRNA expressions between low- and high-risk groups.

### Assessment of the Cuproptosis-Related lncRNAs Signature

Analysis of the ROC curve demonstrated the feasibility and accuracy of employing the riskscore for OS prediction. One-year, three-year, and five-year AUCs were 0.731, 0.723, and 0.747, respectively (Figure 3B). Comparison to other clinicopathological parameters, the riskscore's AUCs in the 5-years ROC of the model were 0.731, demonstrating extraordinarily excellent predictive potential (Figure 3C). The risk model's 10-year C-index was also significantly higher than the average of the other clinical characteristics (Figure 3D). Using Cox regression analysis, we looked at whether the predictive signature could be utilized to predict the outcome of STAD patients independently. Patient survival was found to be significantly predicted by stage and riskscore in a univariate analysis of STAD cases (Figure 3E). Multivariate analysis confirmed the statistical significance of the association between age, stage, and riskscore, even after controlling for confounding variables (Figure 3F).

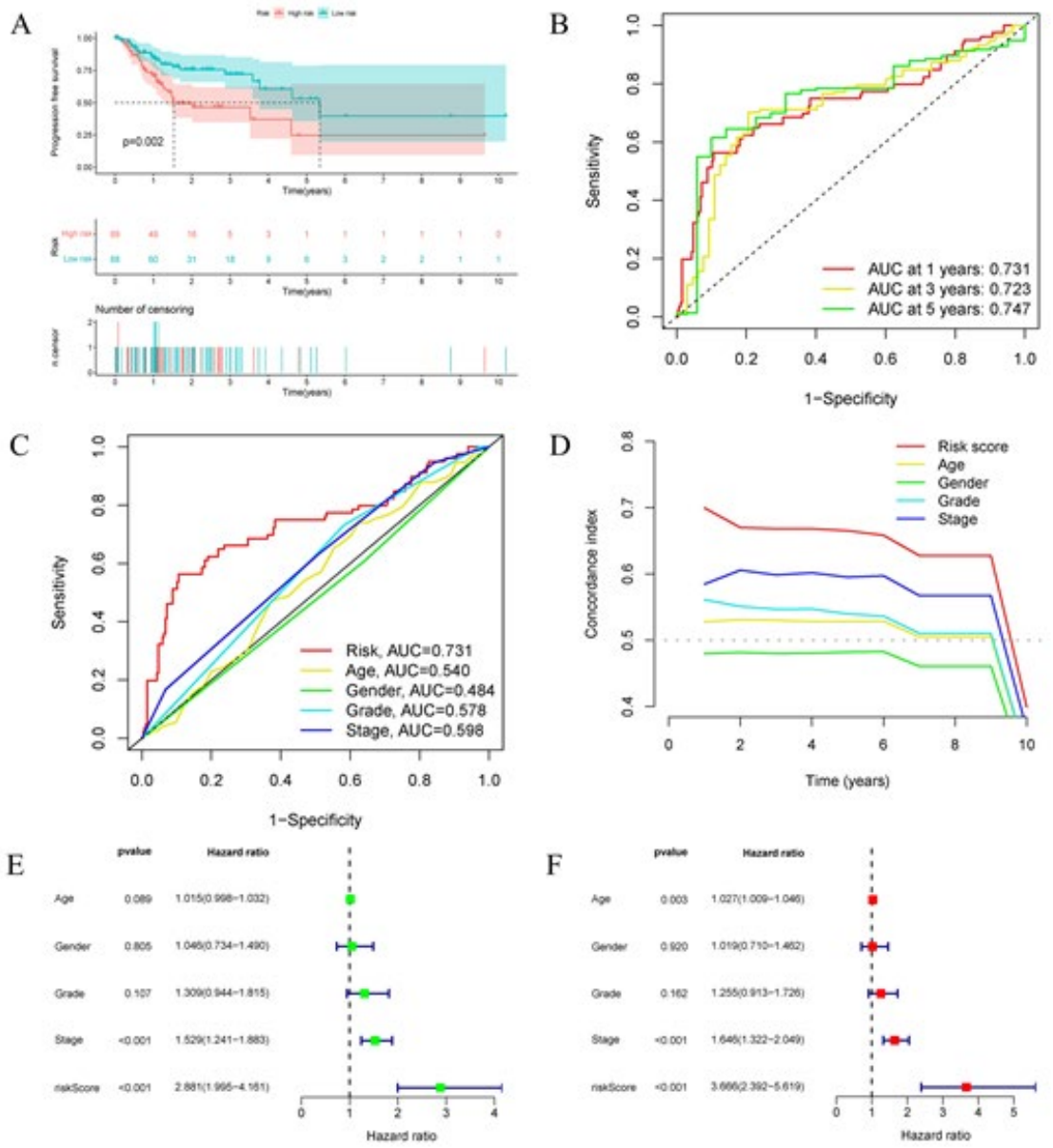


**Figure 3:** A. Comparison of low- and high-risk groups for progression-free survival among STAD patients, as measured by Kaplan-Meier curvest; B. Prediction accuracy over 1, 3, and 5 years using the ROC curves as the risk characteristics; C. Validity of the risk model in comparison to clinicopathologic variables including age, gender, grade, and stage; D. Model risk's C-index curve; E. Univariate Cox regression analysis; F. Multivariate Cox regression analysis.

## Connection Between Different Clinicopathological Variables and Signature

Patients with STAD were categorized by age, gender, stage, T, N, and M to examine the relationship between the predictive signature and prognosis. Our signature performed well in predicting outcomes for those who were younger than 65 ($p < 0.001$), older than 65 ($p < 0.001$), male ($p < 0.001$), female($p < 0.001$), in Grade 1-2 ($p = 0.003$), in Grade 3($p < 0.001$), in M0 ($p < 0.001$), in M1 ($p = 0.025$), in N1-3 ($p < 0.001$), in T3-4 ($p < 0.001$), in Stage 1-2 ($p = 0.007$), in Stage 3-4 ($p < 0.001$), but it was less effective for those in N0 and T1-2 ($p > 0.05$) (Figure 4). Taken together, these data suggest that the predictive signature can be used to predict the prognosis of STAD patients independently of clinicopathological variables.

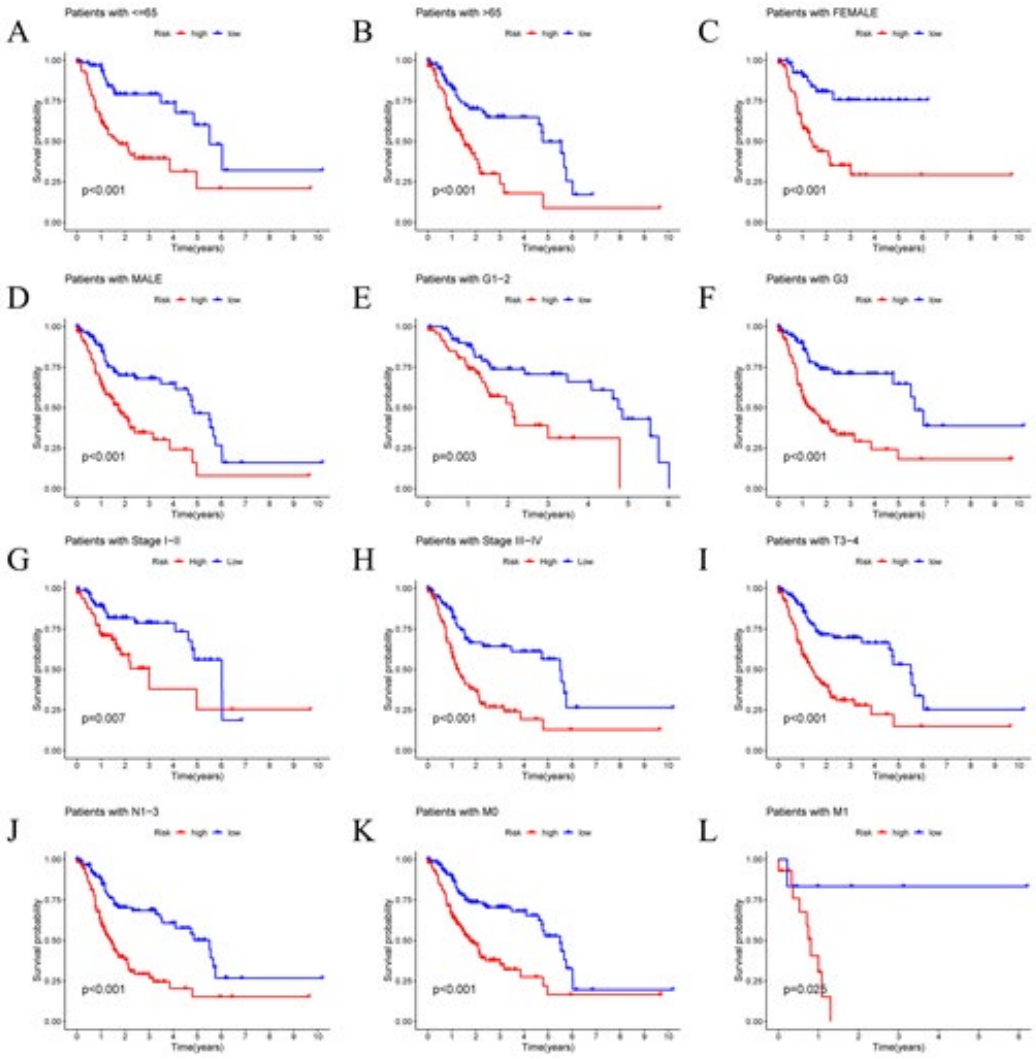


**Figure 4:** Kaplan-Meier survival graphs show differences in OS between high- and low-risk subgroups, stratified by age, gender, grade, and TNM stage.

## Nomogram-Based Validation of the Signature's Prognostic Value in STAD

We developed nomograms using clinical features and riskscore to predict 1-, 3-, and 5-year OS in STAD to verify the prognostic value of cuproptosis-related lncRNA (Figure 5A). Both the data and the calibration curves showed a high degree of agreement (Figure 5B).

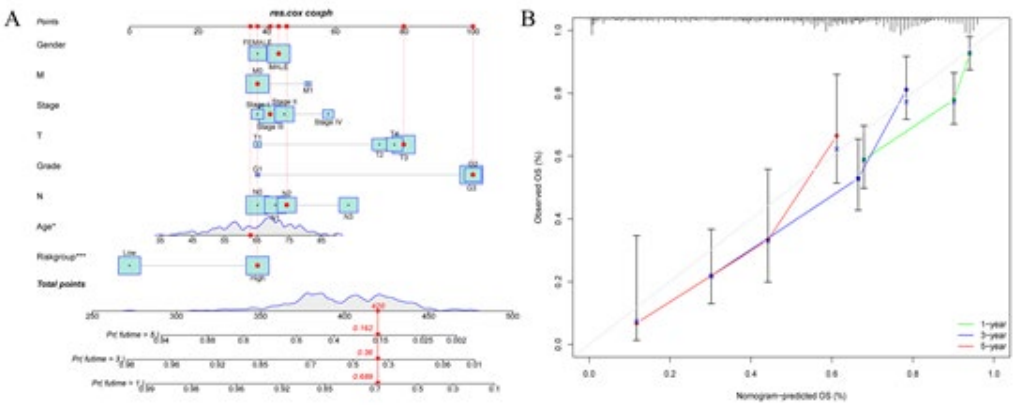


**Figure 5:** A.1-, 3-, or 5-Year Prediction of OS Using a Nomogram; B. Predicting OS over 1, 3, or 5 years using calibration plots.

## The Principal Component Analysis and Functional Enrichment Analyses

We adopted PCA to compare high- and low-risk groups based on four types of expression patterns: total gene expression profiles, cuproptosis genes, cuproptosis-related lncRNAs, and risk models categorized by the expression profiles of 10 cuproptosis-related lncRNAs. The results showed that the 10 lncRNAs linked with cuproptosis had the highest discriminating power between low- and high-risk groups (Figure 6A-D). Gene expression was compared between high-risk and low-risk groups using the lncRNA signature as a basis for differential analysis to gain insight into the prognostic signature's underlying mechanism. To begin, we screened out 202 DEGs using edgeR filtering (p-value < 0.05 and |log2FC| >= 1). We also conducted a GO and KEGG analysis on these DEGs, and the results showed that the DEGs were heavily implicated in biological processes (BP) related to the musculoskeletal system, actomyosin structural organization, and cellular component assembly during morphogenesis. Contractile fiber, myofibril, and plasma membrane raft were identified as cellular components (CC) in the study. Receptor activator activity, ligand activity, and heparin binding were shown to be highly enriched upon examination of molecular function (MF) (Figure 6E). The cGMP-PKG signaling route, the Calcium signaling pathway, and the cAMP signaling pathway were all found to be highly enriched in the data set used for the KEGG analysis (Figure 6F).

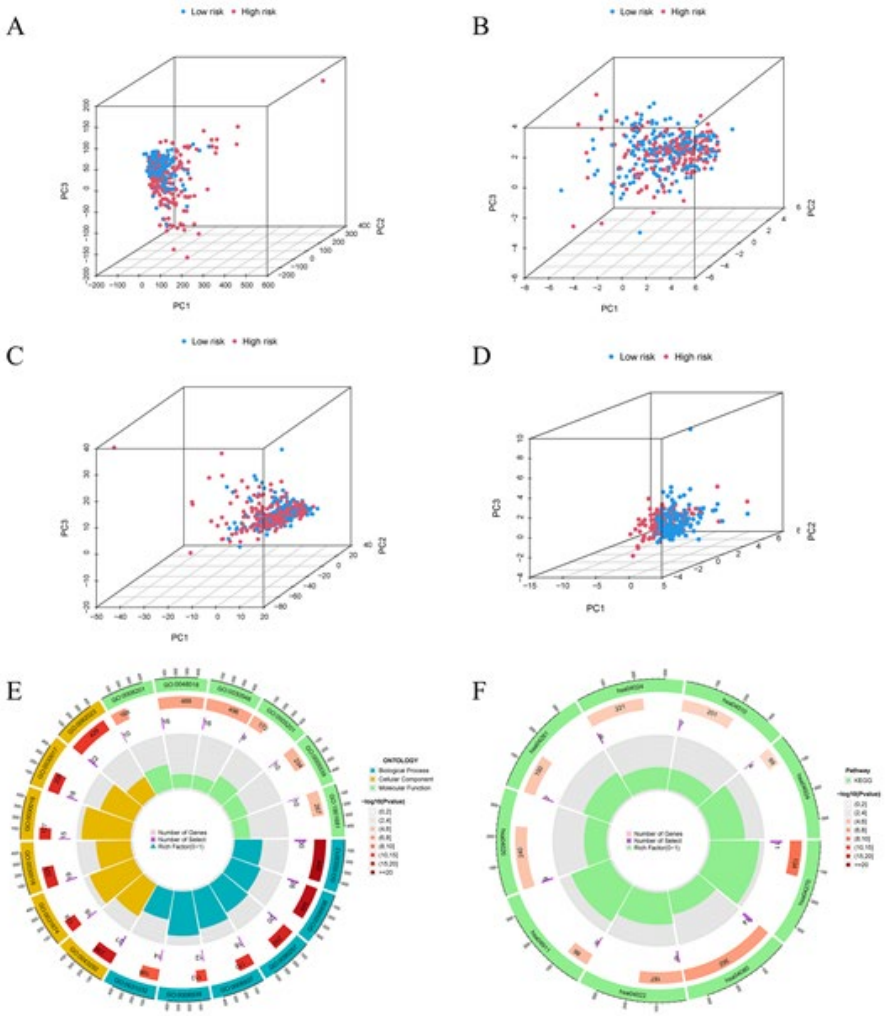


**Figure 6:** A. PCA of all genes; B. PCA of cuproptosis genes; C. PCA of cuproptosis-related lncRNAs; D. PCA of risk lncRNAs; E. GO enrichment analysis; F. KEGG enrichment analysis.

## Immune Cell Infiltration and Immune-Related Function

To further investigate the link between risk scores and immune cells and functions, we analyzed the enrichment scores of ssGSEA for several subgroups of immune cells, associated functions, or pathways. The results showed that high- and low-risk groups had markedly different numbers of activated dendritic cells (aDCs), B cells, CD8 T cells, DCs, immature DCs, macrophages, mast cells, neutrophils, natural killer (NK) cells, plasmacytoid dendritic cells (pDCs), T helper cells, T follicular helper (Tfh) cells, T helper type 1 (Th1) cells, tumor-infiltrating (Figure 7A). Higher scores were found in the high-risk group for the immune functions of antigen-presenting cell (APC) coinhibition, APC costimulation, chemokine receptor (CCR), checkpoint, cytolytic activity, human leukocyte antigen (HLA), inflammation promoting, parainflammation, T cell coinhibition, T cell costimulation, type I IFN response, and type II IFN response (Figure 7B).

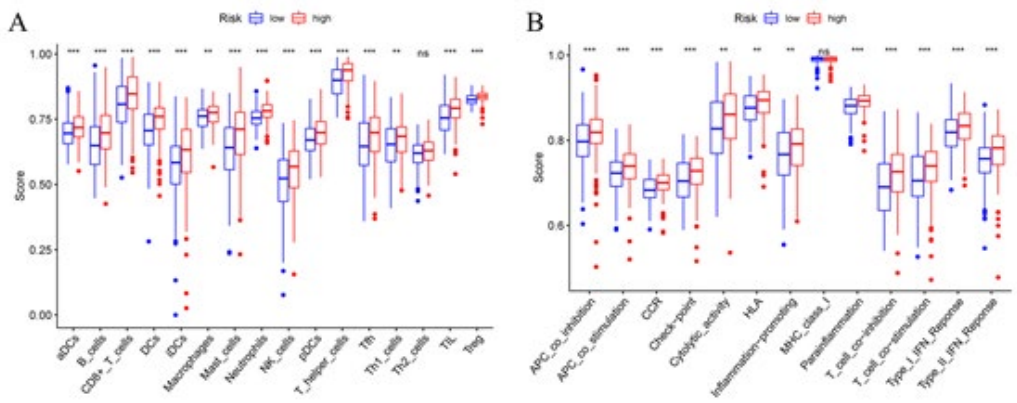


**Figure 7:** A.The ssGSEA method was utilized to determine the relative abundance of 16 distinct types of immune cells in high-risk and low-risk populations respectively; B. Predictive signature's association with 13 immune-related functions. *p < 0.05; **p < 0.01; ***p < 0.001; ns, no significant.

## TMB and TIDE

We obtained information on somatic mutations from the TGCA database and compared the rates at which these mutations occurred in high- and low-risk individuals. TTN, TP53, MUC16, LRP1B, ARID1A, SYNE1, CSMD3, FAT4, FLG, and PCLO were among the top 10 most mutated genes (Figure 8A-B). Most often mutated genes in STAD include TP53, TTN, LRP1B, CSMD3, ARID1A, FAT4, FLG, and PCLO. In terms of TBM, there was a difference between the two groups that could be considered statistically significant (p < 0.05) (Figure 8C). In addition to this, the patients in the cohorts with the highest TMB and the highest risk had the worse prognosis compared to the other groups (Figure 8D-E). When comparing the high-risk and low-risk groups, the high-risk group had considerably higher TIDE scores (Figure 8F).

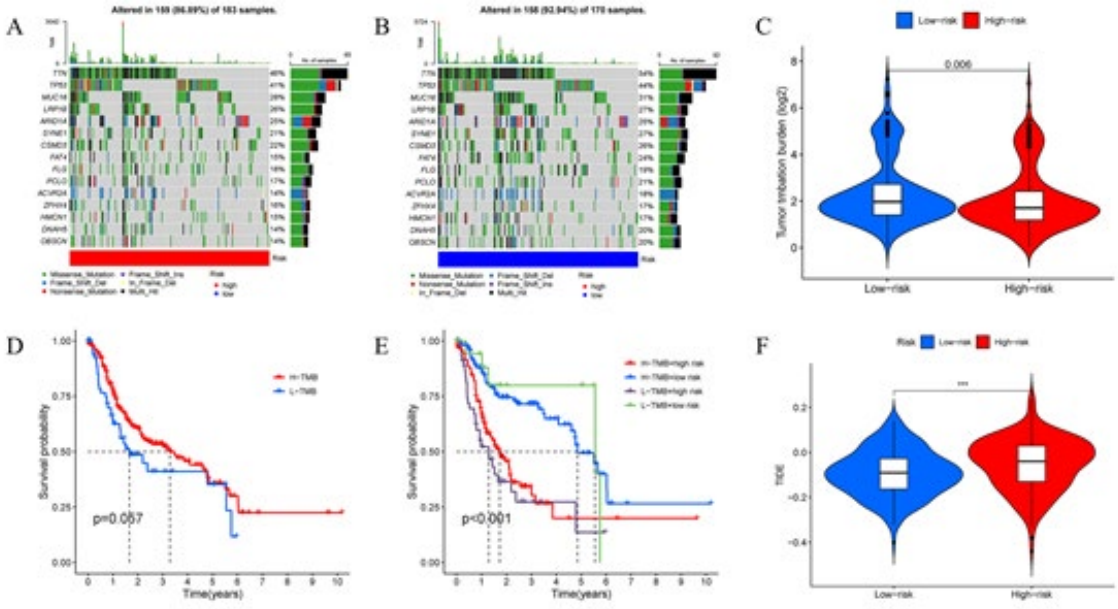


**Figure 8:** A. Waterfall plots of high-risk somatic mutation characteristics; B. Low-risk somatic mutation characteristics; C. Differences in tumor mutation burden (TMB) between low- and high-risk groups; D. Differences in Kaplan-Meier (K-M) survival curves between the two groups; E. Differences in K-M survival curves between the four groups; F. Differences in TIDE scores between the two groups.

## Drug Sensitivity Analysis

Our analysis of IC50 values for a variety of drugs revealed striking differences in drug sensitivity between the low-risk and high-risk groups. The high-risk group had much higher sensitivity to medications like cytarabine, saracatinib, pazopanib, and dasatinib, as seen by their IC50 values being much lower than the low-risk group's (Figure 9A-D). Since the IC50 values for LAQ824, and FH535 were markedly reduced in the low-risk group, we conclude that these drugs are more effective in this population (Figure 9E-F).

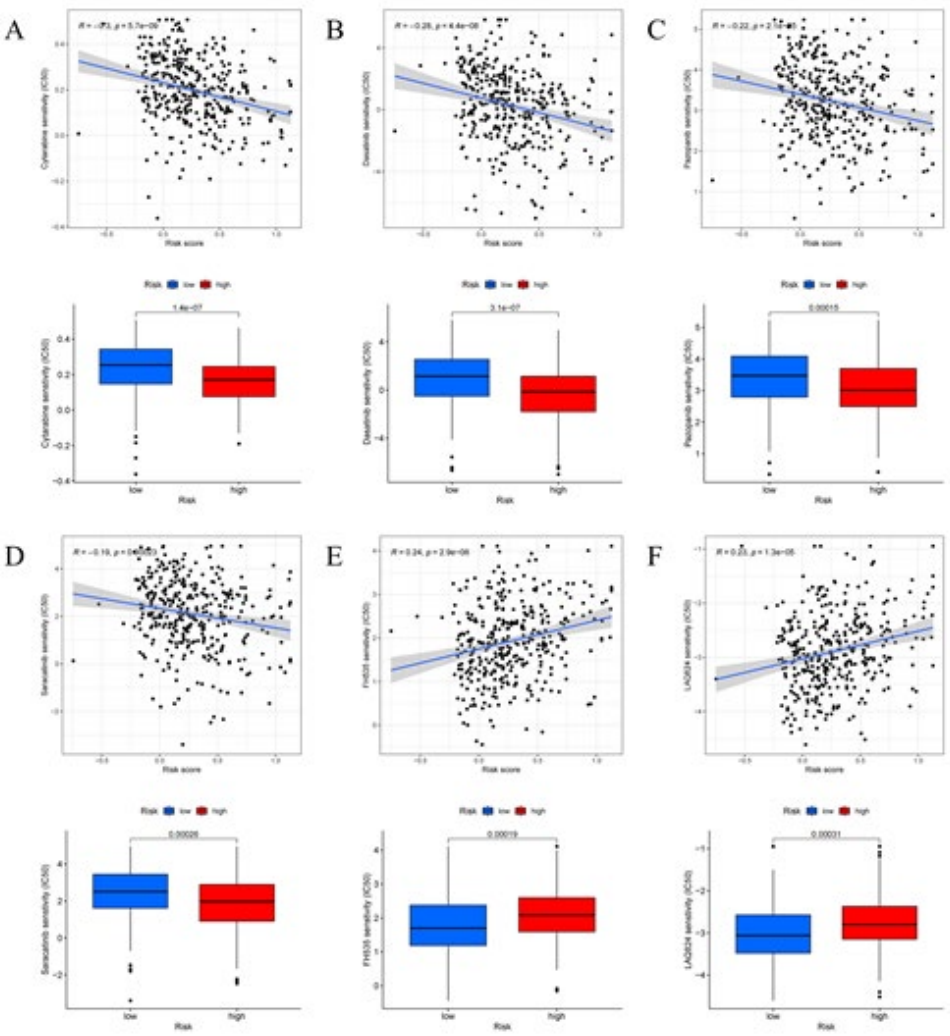


**Figure 9:** Drug sensitivity analysis

## Discussion

"Cuproptosis" is a brand new and distinct method of cell death that occurs as a result of the accumulation of copper within the cell. This method leads to the accumulation of mitochondrial lipoylated proteins as well as the disintegration of Fe-S cluster proteins, both of which ultimately lead to the death of the cell [13, 21]. Copper levels in the serum and tumor tissues of individuals with breast, thyroid, lung, pancreatic, prostate, and oral cavity malignancies have been shown to be dramatically higher in recent studies. This may promote tumor development, growth, angiogenesis, and dissemination [22-29]. For this reason, research pertaining to cuproptosis is desperately required so that it can be better understood.

It has been demonstrated that lncRNAs play a vital regulatory role in STAD. One example is CASC11, which promotes the proliferation, migration, and invasion of gastric cancer cells in vitro by altering the cell cycle pathway, another example is EIF3J-DT, which develops chemoresistance in gastric cancer by activating autophagy [30, 31]. Therefore, we developed a cuproptosis-associated lncRNA signature to assess STAD patients' chances of survival. Overall, we isolated 430 unique lncRNAs associated with cuproptosis. Following this, we used univariate Cox regression analysis and LASSO regression analysis to identify 10 lncRNAs related to cuproptosis that were strongly associated with OS, and we used this signature to predict survival (AC087521.1, AP003498.2, AC069234.5, LINC01094, AC019080.1, BX890604.1, AC005041.3, DPP4-DT, AL356489.2, AL139147.1).

LINC01094 was identified to be overexpressed in many different types of cancerous tissue, most notably glioblastoma, lung adenocarcinoma, and colorectal cancer [32-34]. Poor prognosis is related with high LINC01094 expression in gastric cancer, and this may be due to its association with the epithelial-mesenchymal transition pathway and macrophage infiltration [35, 36]. Furthermore, LINC01094 regulated the signaling axis in a way that enhanced tumorigenic and metastatic characteristics [37]. The remaining lncRNAs that were employed in our signature have biological functions that have only infrequently been reported or investigated in the past.

All of the STAD samples that were a part of the study were randomly divided into the testing set and the training set in an equal ratio so that the practical value of the signature could be demonstrated. According to the AUC of the ROC charts, the signature possessed an adequate level of predictive accuracy across all three sets (train, test, and entire). In addition, we devised a nomogram to forecast the outcome of STAD patients' conditions. The calibration curves demonstrated a very high level of con-

gruence between the observed data and the expectations made. When comparing low- and high-risk groups, PCA revealed that the 10 lncRNAs linked to cuproptosis performed the best. Among the KEGG pathways most heavily represented in cuproptosis-associated lncRNAs were the cGMP-PKG signaling route, the Calcium signaling pathway, and the cAMP signaling pathway. During various stages of human tumor development, both the cGMP-PKG signaling route and the cAMP signaling pathway have been found to contribute to carcinogenesis, survival, tumor growth, and metastasis [38-41].

Using ssGSEA, we found that the high-risk group had significantly greater CD8+ T cells, macrophages, mast cells, and neutrophils. There was a negative correlation between the number of CD8+ T cells infiltrating the bloodstream and the PFS and OS of STAD, according to the studies. Patients with increased CD8+ T cell densities also had higher PD-L1 expression, which may point to an adaptive immunological resistance mechanism [42]. A poor prognosis is observed in patients with gastric cancer who have an abundance of tumor-associated macrophages, which may be due to the EMT phenomenon [43, 44]. Hematogenous metastasis and a poor prognosis in individuals with gastric cancer are linked to high mast cell densities, which in turn are linked to angiogenesis and progression [45, 46]. Neutrophils inside a tumor microenvironment can increase gastric cancer cell migration and invasion by inducing EMT through IL-17a signaling. Patients with STAD who had a significant neutrophil infiltration had a dismal prognosis [47, 48]. High-risk individuals tended to have worse antitumor immunity, as shown by greater HLA and typeI IFN response scores. This was in addition to the already-mentioned increased tumor immune cell infiltration. As a result, diminished antitumor immunity may account for the terrible outcome among the high-risk group.

It has been revealed that TMB can forecast how well tumor patients would respond to immunotherapy [49]. The results of this study showed an inverse relationship between risk score and TMB, which may be connected to immunological effects. Patients' responses to ICI treatment were evaluated using the TIDE methodology [50]. Greater TIDE ratings were seen in the high-risk group compared to the low-risk group, suggesting that the latter may have a diminished response to ICI treatment. In addition, Our findings suggested that Cytarabine, Saracatinib, Pazopanib, and Dasatinib would be beneficial for patients in the high-risk group.

Therefore, the 10lncRNA signature may be used as a predictive tool for estimating the probability of survival for STAD patients classified according to several clinicopathological risk factors. On the other hand, there are caveats to our study. We need information from other databases for external validation to evaluate the predictive signature thoroughly. Furthermore, experimental confirmation of the mechanism of the cuproptosis-related lncRNAs in STAD is required.

## Authors' Contributions

Contributions: (I) Conception and design: Qi Ma, Yuan Hui, Bang-Rong Huang; (II) Administrative support: Bang-Rong Huang, Bin-Feng Yang; (III) Provision of study materials or patients: Bang-Rong Huang; (IV) Collection and assembly of data: Qi Ma, Yuan Hui, Jing-Xian Li, Da-You Ma; (V) Data analysis and interpretation: Qi Ma, Yuan Hui, Jing-Xian Li; (VI) Manuscript writing: All authors; (VII) Final approval of manuscript: All authors.


## Funding

Gansu Province Science and Technology Foundation (No. 18JR-2FA001); Gansu Province Education Science and Technology Innovation Project (No. 2022CXZX-756).


## Availability of Data and Materials

The raw data of this study is derived from the TCGA database (https://portal.gdc.cancer.gov/) which is publicly available databases.

## Declarations

Ethical approval and Consent to participate

This article does not contain any studies with human participants or animals performed by any of the authors.

Consent for publication

All authors consent to the publication of this study.

Competing interests

No competing interests.

## References


1. Thrift, A. P., & El-Serag, H. B. (2020). Burden of gastric cancer. Clinical Gastroenterology and Hepatology, 18(3), 534-542.
2. Bray, F., Ferlay, J., Soerjomataram, I., Siegel, L. R., Torre, A. L., & Ahmedin, D. V. M. GLOBOCAN estimates of incidence and mortality worldwide for 36 cancers in 185 countries. Global cancer statistics 2018.
3. Joshi, S. S., & Badgwell, B. D. (2021). Current treatment and recent progress in gastric cancer. CA: a cancer journal for clinicians, 71(3), 264-279.
4. Tan, Z. (2019). Recent advances in the surgical treatment of advanced gastric cancer: a review. Medical science monitor: international medical journal of experimental and clinical research, 25, 3537.
5. Wang, N., & Liu, D. (2021). Identification and validation a necroptosis related prognostic signature and associated regulatory axis in stomach adenocarcinoma. OncoTargets and therapy, 14, 5373.
6. Nie, K., Deng, Z., Zheng, Z., Wen, Y., Pan, J., Jiang, X., ... & Li, P. (2020). Identification of a 14-lncRNA signature and construction of a prognostic nomogram predicting overall survival of gastric cancer. DNA and Cell Biology, 39(9), 1532-1544.
7. Sun, J., Jiang, Q., Chen, H., Zhang, Q., Zhao, J., Li, H., ... & Sun, Y. (2021). Genomic instability-associated lncRNA signature predicts prognosis and distinct immune landscape in gastric cancer. Annals of Translational Medicine, 9(16).
8. Wang, Y., Zhang, X., Dai, X., & He, D. (2021). Applying immune-related lncRNA pairs to construct a prognostic signature and predict the immune landscape of stomach adenocarcinoma. Expert Review of Anticancer Therapy, 21(10), 1161-1170.
9. Ge, E. J., Bush, A. I., Casini, A., Cobine, P. A., Cross, J.

R., DeNicola, G. M., ... & Chang, C. J. (2022). Connecting copper and cancer: from transition metal signalling to metalloplasia. Nature Reviews Cancer, 22(2), 102-113.
10. Ishida, S., Andreux, P., Poitry-Yamate, C., Auwerx, J., & Hanahan, D. (2013). Bioavailable copper modulates oxidative phosphorylation and growth of tumors. Proceedings of the National Academy of Sciences, 110(48), 19507-19512.
11. Blockhuys, S., Celauro, E., Hildesjö, C., Feizi, A., Stål, O., Fierro-González, J. C., & Wittung-Stafshede, P. (2017). Defining the human copper proteome and analysis of its expression variation in cancers. Metallomics, 9(2), 112-123.
12. Park, K. C., Fouani, L., Jansson, P. J., Wooi, D., Sahni, S., Lane, D. J., ... & Richardson, D. R. (2016). Copper and conquer: copper complexes of di-2-pyridylketone thiosemicarbazones as novel anti-cancer therapeutics. Metallomics, 8(9), 874-886.
13. Tsvetkov, P., Coy, S., Petrova, B., Dreishpoon, M., Verma, A., Abdusamad, M., ... & Golub, T. R. (2022). Copper induces cell death by targeting lipoylated TCA cycle proteins. Science, 375(6586), 1254-1261.
14. Davis, C. I., Gu, X., Kiefer, R. M., Ralle, M., Gade, T. P., & Brady, D. C. (2020). Altered copper homeostasis underlies sensitivity of hepatocellular carcinoma to copper chelation. Metallomics, 12(12), 1995-2008.
15. Liu, S. J., & Lim, D. A. (2018). Modulating the expression of long non-coding RNA s for functional studies. EMBO reports, 19(12), e46955.
16. Esposito, R., Bosch, N., Lanzós, A., Polidori, T., Pulido-Quetglas, C., & Johnson, R. (2019). Hacking the cancer genome: profiling therapeutically actionable long non-coding RNAs using CRISPR-Cas9 screening. Cancer cell, 35(4), 545-557.
17. Kim, J., Piao, H. L., Kim, B. J., Yao, F., Han, Z., Wang, Y., ... & Ma, L. (2018). Long noncoding RNA MALAT1 suppresses breast cancer metastasis. Nature genetics, 50(12), 1705-1715.
18. Ransohoff, J. D., Wei, Y., & Khavari, P. A. (2018). The functions and unique features of long intergenic non-coding RNA. Nature reviews Molecular cell biology, 19(3), 143-157.
19. Huarte, M. (2015). The emerging role of lncRNAs in cancer. Nature medicine, 21(11), 1253-1261.
20. Luo, J., Langer, L. F., & Liu, J. (2019). A novel role of LncRNA in regulating tumor metabolism and angiogenesis under hypoxia. Cancer Communications, 39(1), 1-3.
21. Tang, D., Chen, X., & Kroemer, G. (2022). Cuproptosis: a copper-triggered modality of mitochondrial cell death. Cell Research, 32(5), 417-418.
22. Basu, S., Singh, M. K., Singh, T. B., Bhartiya, S. K., Singh, S. P., & Shukla, V. K. (2013). Heavy and trace metals in carcinoma of the gallbladder. World Journal of Surgery, 37(11), 2641-2646.
23. Ding, X., Jiang, M., Jing, H., Sheng, W., Wang, X., Han, J., & Wang, L. (2015). Analysis of serum levels of 15 trace elements in breast cancer patients in Shandong, China. Environmental Science and Pollution Research, 22(10), 7930-7935.
24. Baltaci, A. K., Dundar, T. K., Aksoy, F., & Mogulkoc, R. (2017). Changes in the serum levels of trace elements before and after the operation in thyroid cancer patients. Biological trace element research, 175(1), 57-64.
25. Stepien, M., Jenab, M., Freisling, H., Becker, N. P., Czuban, M., Tjønneland, A., ... & Hughes, D. J. (2017). Pre-diagnostic copper and zinc biomarkers and colorectal cancer risk in the European Prospective Investigation into Cancer and Nutrition cohort. Carcinogenesis, 38(7), 699-707.
26. Zhang, X., & Yang, Q. (2018). Association between serum copper levels and lung cancer risk: A meta-analysis. Journal of International Medical Research, 46(12), 4863-4873.
27. Chen, F., Wang, J., Chen, J., Yan, L., Hu, Z., Wu, J., ... & He, B. (2019). Serum copper and zinc levels and the risk of oral cancer: A new insight based on large-scale case–control study. Oral diseases, 25(1), 80-86.
28. Saleh, S. A., Adly, H. M., Abdelkhaliq, A. A., & Nassir, A. M. (2020). Serum levels of selenium, zinc, copper, manganese, and iron in prostate cancer patients. Current urology, 14(1), 44-49.
29. Oliveri, V. (2022). Selective Targeting of Cancer Cells by Copper Ionophores: An Overview. Frontiers in Molecular Biosciences, 9.
30. Zhang, L., Kang, W., Lu, X., Ma, S., Dong, L., & Zou, B. (2018). LncRNA CASC11 promoted gastric cancer cell proliferation, migration and invasion in vitro by regulating cell cycle pathway. Cell cycle, 17(15), 1886-1900.
31. Luo, Y., Zheng, S., Wu, Q., Wu, J., Zhou, R., Wang, C., ... & Liao, W. (2021). Long noncoding RNA (lncRNA) EIF3J-DT induces chemoresistance of gastric cancer via autophagy activation. Autophagy, 17(12), 4083-4101.
32. Dong, X., Fu, X., Yu, M., & Li, Z. (2020). Long intergenic non-protein coding RNA 1094 promotes initiation and progression of glioblastoma by promoting microRNA-577-regulated stabilization of brain-derived neurotrophic factor. Cancer Management and Research, 12, 5619.
33. Wu, Z., Bai, X., Lu, Z., Liu, S., & Jiang, H. (2022). LINC01094/SPI1/CCL7 Axis Promotes Macrophage Accumulation in Lung Adenocarcinoma and Tumor Cell Dissemination. Journal of immunology research, 2022, 6450721-6450721.
34. Zhang, G., Gao, Y., Yu, Z., & Su, H. (2022). Upregulated long intergenic non-protein coding RNA 1094 (LINC01094) is linked to poor prognosis and alteration of cell function in colorectal cancer. Bioengineered, 13(4), 8526-8537.
35. Ye, Y., Ge, O., Zang, C., Yu, L., Eucker, J., & Chen, Y. (2022). LINC01094 Predicts Poor Prognosis in Patients With Gastric Cancer and is Correlated With EMT and Macrophage Infiltration. Technology in cancer research & treatment, 21, 15330338221080977.
36. Jiang, Y., Zhang, H., Li, W., Yan, Y., Yao, X., & Gu, W. (2020). FOXM1-activated LINC01094 promotes clear cell renal cell carcinoma development via microRNA 224-5p/CHSY1. Molecular and cellular biology, 40(3), e00357-19.
37. Li, X. X., & Yu, Q. (2020). Linc01094 accelerates the growth and metastatic-related traits of glioblastoma by sponging miR-126-5p. OncoTargets and therapy, 13, 9917.
38. Xiang, T., Yuan, C., Guo, X., Wang, H., Cai, Q., Xiang, Y., ... & Liu, G. (2021). The novel ZEB1-upregulated protein PRTG induced by Helicobacter pylori infection promotes gastric carcinogenesis through the cGMP/PKG signaling

pathway. Cell death & disease, 12(2), 1-15.
39. Jiang, K., Yao, G., Hu, L., Yan, Y., Liu, J., Shi, J., ... & Piao, H. (2020). MOB2 suppresses GBM cell migration and invasion via regulation of FAK/Akt and cAMP/PKA signaling. Cell death & disease, 11(4), 1-14.
40. Cheng, Y., Gao, X. H., Li, X. J., Cao, Q. H., Zhao, D. D., Zhou, J. R., ... & Yang, Y. (2018). Depression promotes prostate cancer invasion and metastasis via a sympathetic-cAMP-FAK signaling pathway. Oncogene, 37(22), 2953-2966.
41. Lv, Y., Wang, X., Li, X., Xu, G., Bai, Y., Wu, J., ... & Wang, L. (2020). Nucleotide de novo synthesis increases breast cancer stemness and metastasis via cGMP-PKG-MAPK signaling pathway. PLoS biology, 18(11), e3000872.
42. Thompson, E. D., Zahurak, M., Murphy, A., Cornish, T., Cuka, N., Abdelfatah, E., ... & Kelly, R. J. (2017). Patterns of PD-L1 expression and CD8 T cell infiltration in gastric adenocarcinomas and associated immune stroma. Gut, 66(5), 794-801.
43. Zhang, J., Yan, Y., Yang, Y. A., Wang, L., Li, M., Wang, J., ... & Wang, J. (2016). High infiltration of tumor-associated macrophages influences poor prognosis in human gastric cancer patients, associates with the phenomenon of EMT. Medicine, 95(6).
44. Su, C. Y., Fu, X. L., Duan, W., Yu, P. W., & Zhao, Y. L. (2018). High density of CD68+ tumor-associated macrophages predicts a poor prognosis in gastric cancer mediated by IL-6 expression. Oncology letters, 15(5), 6217-6224.
45. Ribatti, D., Guidolin, D., Marzullo, A., Nico, B., Annese, T., Benagiano, V., & Crivellato, E. (2010). Mast cells and angiogenesis in gastric carcinoma. International journal of experimental pathology, 91(4), 350-356.
46. Ammendola, M., Marech, I., Sammarco, G., Zuccalà, V., Luposella, M., Zizzo, N., ... & Ranieri, G. (2015). Infiltrating mast cells correlate with angiogenesis in bone metastases from gastric cancer patients. International Journal of Molecular Sciences, 16(2), 3237-3250.
47. Li, S., Cong, X., Gao, H., Lan, X., Li, Z., Wang, W., ... & Zhao, Y. (2019). Tumor-associated neutrophils induce EMT by IL-17a to promote migration and invasion in gastric cancer cells. Journal of Experimental & Clinical Cancer Research, 38(1), 1-13.
48. Cupp, M. A., Cariolou, M., Tzoulaki, I., Aune, D., Evangelou, E., & Berlanga-Taylor, A. J. (2020). Neutrophil to lymphocyte ratio and cancer prognosis: an umbrella review of systematic reviews and meta-analyses of observational studies. BMC medicine, 18(1), 1-16.
49. Chalmers, Z. R., Connelly, C. F., Fabrizio, D., Gay, L., Ali, S. M., Ennis, R., ... & Frampton, G. M. (2017). Analysis of 100,000 human cancer genomes reveals the landscape of tumor mutational burden. Genome medicine, 9(1), 1-14.
50. Wang, Q., Li, M., Yang, M., Yang, Y., Song, F., Zhang, W., ... & Chen, K. (2020). Analysis of immune-related signatures of lung adenocarcinoma identified two distinct subtypes: implications for immune checkpoint blockade therapy. Aging (albany NY), 12(4), 3312.